INVESTIGATION OF A STOP-FOLD TILTROTOR

A Thesis
Presented to
The Academic Faculty

by

Jeff Bosworth

In Partial Fulfillment
of the Requirements for the Degree
Master of Science in Aerospace Engineering in the
School of Aerospace Engineering

Georgia Institute of Technology
August 2009

INVESTIGATION OF A STOP-FOLD TILTROTOR

Approved by:

Professor Dewey Hodges, Advisor
School of Aerospace Engineering
Georgia Institute of Technology

Professor Lakshmi Sankar
School of Aerospace Engineering
Georgia Institute of Technology

Professor Olivier Bauchau
School of Aerospace Engineering
Georgia Institute of Technology

Date Approved: June 16 2009

To my parents,

Mark and Diane Bosworth,

without whose support,

my achievements would have been impossible.

TABLE OF CONTENTS

LIST OF FIGURES

SUMMARY

In 1967 the US Air Force solicited proposals for "low-disc-loading [Vertical Takeoff and Landing] configurations suitable for high speed flight"[1]. Bell Helicopter elected to respond with a proposal after initial analysis on configurations including a stopped edgewise disc and a trail rotor. They concluded that a folding proprotor design would best meet the requirements laid forth[1]. Initial analysis work began on this folding proprotor (stop-fold) design in the same year and concluded in 1972 with a full scale 25 foot diameter pylon and rotor assembly wind tunnel test at the NASA-Ames Large Scale Wind Tunnel. The project was concluded at this point and never resulted in a production or research aircraft.

The original proposed stop-fold tiltrotor design by Bell Helicopter allowed for vertical takeoff and landing, a transition sequence rotating the pylon rotor assembly from helicopter to airplane mode, a conversion sequence during which the rotor stopped and blades folded along the pylon, and a transition from prop thrust to auxiliary jet engine power while the rotor was being stopped[2]. This configuration effectively removes the high-speed restraints typical of a prop-driven aircraft and instead opens a flight envelope comparable to a fixed-wing jet.

This project entails both the simulation and basic analysis of the stop-fold concept with special attention to frequency responses and potential coupling between modes.

CHAPTER I

BACKGROUND

1.1 Original Design

Bell Helicopter responded to an Air Force request in 1967 for a low disc loading VTOL aircraft with their proposed stop-fold tiltrotor design. This aircraft centered around a three-bladed, 25 foot diameter rotor with the unique feature of having blades able to be folded back 90 degrees along the pylon for storage during high-speed flight. The rotor design was based on the Bell Model 627 rotor and was modified to include joints for both feathering and folding and featured a gimbaled hub. The hub design was further modified to include a flap lock to be engaged as the rotor slowed to prevent excess flapping. The proposed stop-fold design was controlled with a swash plate and pitch link assembly [2].

1.1.1 Conversion Sequence

For the purposes of this paper, references to the conversion sequence will refer to motion involving the folding of the rotor blades back along the pylon as opposed to the traditional tiltrotor conversion sequence involving the rotor shift from helicopter mode to airplane mode. Figure 1 summarizes the entire stop-fold sequence as a flowchart with the details of each step included. During forward flight in airplane mode, the aircraft is designed to begin the conversion sequence in a low to mid airspeed range approximately 140–170 kts [1].

1.1.2 Stop Sequence

To initiate the rotor stop, power is initially routed from the rotors to the jet engine bypass fan to being reducing rotor torque. When the rotor has reached approximately

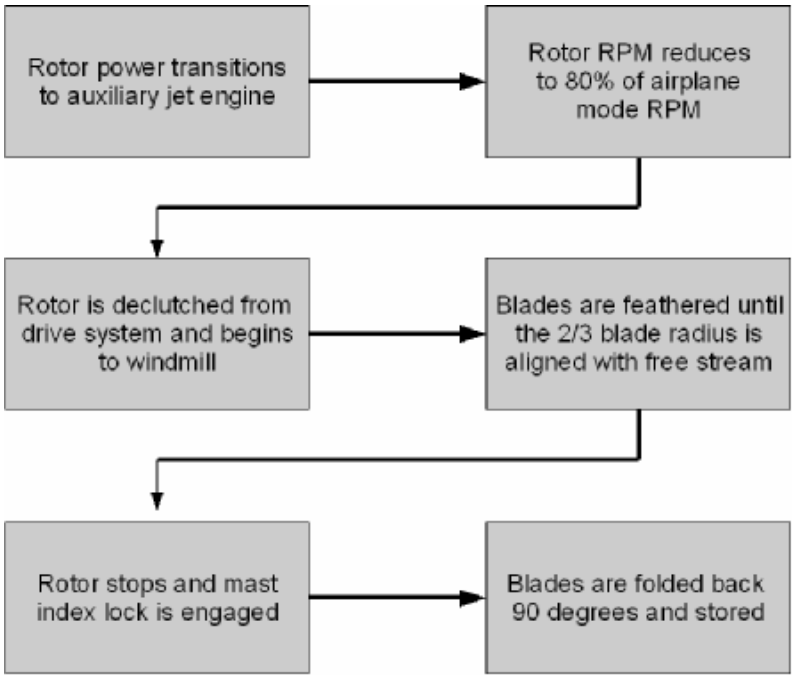

Figure 1: Conversion Sequence Flowchart

80% of airplane mode RPM the rotor flap lock is engaged to prevent excess flapping and damage to the wing as the engine slows. Once the flap lock has been engaged, the rotor can be declutched from the drive system to windmill. While rotating freely, the rotor is stopped by raising the collective and feathering the blades until the two-thirds radius is aligned with the free stream. This two-thirds point was calculated and confirmed experimentally for the blade configuration to be the point about which nearly no moments were generated with respect to the pylon centerline [1]. Once the rotor has slowed to 0-3 RPM the mast can be indexed and locked into place.

Original investigations conducted by Bell Helicopter found that a fast feather rate, approximately 2 seconds from windmilling to fully feathered, limited the buildup of vibratory loads on the system. During initial testing, "Hardware limitations prevented evaluation of a range of feathering rates,"[1] and it would be reasonable to expect to use the proposed model to evaluate a range of feathering rates.

1.1.3 Fold Sequence

Following the stop sequence, the blades must be folded back along the pylon. The fold sequence is an actuator driven fold to allow both folding and unfolding motions during flight. Wind tunnel testing on two configurations of fold (edgewise and flat-wise) indicated reduced drag in the edgewise configuration [5]. Additionally, the blades needed to be locked into place along the pylon with the use of inflatable bladders to prevent excess motion during high-speed operation [2].

The entire stop-fold sequence is designed to be entirely reversible to allow the aircraft to decelerate from jet cruise speed, unlock and unfold the blades, deploy the blades using the fold actuator, and restart the prop by engaging the drive system clutch and reducing collective.

1.2 Early Analysis

During the initial investigation into the stop-fold tiltrotor concept another project was initiated along with the stop-fold tiltrotor to create an analysis program capable of handling a stopped rotor. According to the engineering manual for this program with respect to the calculation of aerodynamic loads, "No provision is made for the effect on blade loads of the type of hub, mass distribution of the blades, or aeroelastic feedback"[3]. Additionally, most of the analysis was based on a set of uncoupled equations rather than being based on eigen analysis.

After initial testing on the stop-fold tiltrotor, Bell Helicopter discovered an unpredicted interference effect between the rotor and leading edge of the wing as the blades passed in front during airplane mode [4]. After the conclusion of the wind tunnel project, an effort was initiated to account for and model this perceived interference effect and study the stability of the system. However, even this analysis was very limited in the assumptions made [5]:

- 2-D incompressible airfoil theory is sufficient for representing the aerodynamics

for the rotor blades and wing. In addition, the wing and rotor blades can be represented by a finite number of swanwise strips.

- The wing section in segment n can be represented by a symmetrical Joukowsky airfoil whose thickness to chord ratio is matched to that of the wing being analyzed.

- The rotor blade section in segment n can be represented by a concentrated vortex representing the bound circulation of the blade.

- Separated flow effects, such as spanwise flow on the rotor blades and wing, and viscous effects in the rotor slipstream are not significant.

As the field of high-speed rotorcraft continues to develop, more and more tools are becoming available to design these aircrafts. As the tools and modeling methods become more advanced, so too do the aircraft being produced. In a large part, these advances are the primary motivation behind this investigation.

CHAPTER II

MOTIVATION

As part of a review of several approaches to high-speed rotorcraft, Talbot, Phillips, and Totah of the NASA Ames Research Center suggested that what they refer to as the folding tiltrotor (the stop-fold tiltrotor) has the highest speed potential of all the aircraft they reviewed due to the fundamental fact that high-speed flight is not achieved by rotor propulsion[6]. Other concepts in their review included a variable diameter tiltrotor, two stopped rotor concepts, and a rotor-in-wing concept.

Talbot, Phillips, and Totah concluded, after inspection of trade studies and current technology, that "Current technology values for empty weight, propulsive efficiency, airfract drag, etc., lead to high-mission gross weight for high-speed rotorcraft compared to fixed wing aircraft"[6]. They concluded that these high gross weights are a result of empty weight and fuel fractions mainly due to higher airframe drag or "poor propulsive efficiency"[6]. The stop-fold tiltrotor has the potential to overcome several of these obstacles by the nature of its design. By using an auxiliary engine, propulsive efficiency can be maximized in cruise simply by engine selection. Airframe drag is greatly reduced by folding and storing the blades during high-speed operation. Each of these features yields the stop-fold tiltrotor a highly viable future technology for high-speed rotorcraft.

In 1999, Peretz P. Friedmann responded to an article written by H. Ashley[9] in which he claimed that very gradual process in the field of aeroelasticity had occurred since 1970. Friedmann responded by claiming that while the area of fixed wing aeroelasticity had not made many major strides, rotary wing aeroelasticity has made very large strides since the 1970s [7]. Among the problems being addressed in the last

30 years is the aeroelastic response of blades to unsteady loads inherent to rotorcraft.

Due to the lack of appropriate research tools and the potential for future operation in the field of high-speed rotorcraft design, it is the opinion of the author that the stop-fold tiltrotor is a concept worthy of future research.

CHAPTER III

SCOPE

In an effort to capture the important effects that make the stop-fold design unique from existing aircraft, this project focused on simulating the actual stop-fold sequence as it relates to both structural dynamics and aeroelastic effects. It was not the aim of this project to attempt to duplicate the results of the wind tunnel test at NASA-Ames but rather to use an approximation of that wind tunnel model as a baseline for creating a representative stop-fold model to be used for future work.

The intention of this project was to further the state of current research into the stop-fold concept and allow for future expansions upon this work. To this end, special attention was be placed on facilitating future work by using an object-oriented coding structure to allow for the replacement of rigid bodies with more realistic beams or spring mass assemblies. Additional provisions have also been made to facilitate the addition of a wing mount or entire aircraft attached to the pylon-rotor assembly.

3.1 Model

The primary goal of this project was to create a structural model of the stop-fold pylon and rotor assembly. It is capable of simulating the conversion sequence. The model includes a flexibly mounted pylon, a hub rotor assembly, and a control system consisting of a swashplate, pitch link, and pitch horn. The model also includes methods for simulating collective pitch and blade fold. The work was centered upon providing a tool capable of expanding on the previous work done by Bell Helicopter between 1967 and 1972 rather than attempting to recreate their findings.

The pylon, including the drive shaft, was modeled as a rigid body mounted on two torsional springs and one linear spring aligned in the axial direction to simulate

being mounted on a wing or test stand. The torsional springs will generate moments normal to the axial direction and tuned iteratively to be representative of values given in Reference [1], the final report from the wind tunnel test.

The blades, as mentioned, will be modeled as flexible beams mounted on a rigid hub. While the hub will be modeled as a rigid body, it will be mounted in a similar manner to the pylon but on only two torsional springs rather than two torsional springs and one linear spring. These spring stiffnesses can be modified to represent the flap lock engaged or disengaged depending on the simulation.

The control system will be modeled primarily as rigid bodies. The control system stiffness will be accounted for in the blade torsion mode via a linear spring aligned with the pitch link vertical direction. This spring can be tuned in a similar manner, iteratively, as the pylon mount springs.

3.2 Structural Dynamics

The model was to be used primarily as a structural dynamics analysis tool. The morphing geometry of the stop-fold tiltrotor presents a unique situation from a rotor dynamics perspective as both the natural frequencies and excitation frequencies can shift during the transition period. The model should capture these transition-related effects to better predict unstable couplings between the rotor and other system such as pylon or wing assemblies. Prediction of the failure modes through natural frequency couplings and mitigating their risk is also a dynamic analysis covered by the model.

3.3 Aerodynamics

While a CFD analysis of the fold sequence is beyond the scope of this project, the selection of DYMORE will allow a coupled model at a later date for future work. For the purpose of this analysis, fairly simplified aerodynamics were used to generate the aeroelastic loads.

3.4 Expectations Summary

At the outset of this project, it was expected to have a working DYMORE model capable of simulating the dynamics of a flexibly mounted pylon, a control system including swash plate and pitch links, and associated rotor hub and blades undergoing a fold sequence maneuver. The analysis focused primarily on the structural dynamics and response of the system to look for structural instabilities as the natural frequencies shift during the morphing procedures. Secondarily the analysis was used to look at the aeroelastic response of the system undergoing the same fold sequence to look for other potential instabilities. Lastly, the model was be expected to be object oriented in nature to facilitate the coupling of future models or refined components to aid in the future research on the stop-fold tiltrotor.

CHAPTER IV

DYMORE COMPONENTS

Being a multibody structural dynamics code, DYMORE employs an extremely large number of components available to build a model. While complex, the stop-fold DYMORE model still only uses a small number of possible components. The components used to build the model, along with their basic functions, are detailed here.

4.1 Structural Elements

- Rigid Body - A rigid body is considered an infinitely stiff element by DYMORE. Rigid bodies comprise most of the stop-fold model as the important dynamic characteristics are being captured primarily by joints and springs. Mass properties may optionally be defined for rigid bodies including inertia properties.

- Associated Rigid Body - To facilitate connections to more than two bodies, an associated rigid body acts as an extension of the parent rigid body. While the base point must match that of the parent rigid body, the second connection point can be something entirely different to allow for multiple connections. The associated rigid body is used in the stop-fold model to allow connection of the yoke to the hub, the blade and the pitch horn.

- Beam - A beam element is a structural element containing finite mass, stiffness, and inertia properties. Some of the required parameters include a weight per inch, stiffness parameters, moments of inertia, and center of mass offsets. These parameters are typically expressed (as is the case in the stop-fold model) in table format. Additionally, DYMORE handles the sharp parameter changes typical of rotor blades by utilizing a Gauss point property smoothing algorithm. This

algorithm is "based on conservation arguments for mass properties and energy considerations for stiffness properties."[8]

- Revolute Joint - The revolute joint permits rotation between two bodies about a single axis of rotation common to both bodies. The stop-fold model utilizes the revolute joint for the feathering joint, fold joint, and the joint near the ground mount to permit rotor rotation.

- Universal Joint - The universal joint permits rotation between two bodies about two axes of rotation. The stop-fold model utilizes the universal joint for the ground pylon mount, the connection between the hub and the shaft to permit flapping, and the connection between the pitch link and the swashplate.

- Prismatic Joint - The prismatic joint permits displacement between two bodies along a single axis common to both bodies. The stop-fold model utilizes the prismatic joint for the connection between the swashplate and shaft as well as the break in the middle of the pitch link to accommodate the control system stiffness approximation.

- Spherical Joint - The spherical joint permits rotation between two bodies about any direction. The only spherical joint in the stop-fold model connects the top of the pitch link to the pitch arm.

- Spring - The spring element in DYMORE must be associated with a relative rotation or displacement between two bodies to function correctly. There are several springs in the stop-fold model related to the universal joint at the hub-shaft junction, the universal joint at the ground mount and the prismatic joint separating the pitch link components.

4.2 Aerodynamic Elements

- Aerodynamic Interface - The aerodynamic interface is the defining element in which the interaction of each of the other aerodynamic elements is governed. This element combines ambient air properties with the inflow model and the lifting lines to generate the aerodynamic loads.

- Lifting Line - The lifting line element is a fairly simple way of associating aerodynamic properties with a beam element. For this stop-fold model, the blades are modeled as beams with associated lifting lines.

- Rotor - The rotor element collects specified lifting lines to be included in the inflow model.

- Air Properties - A fairly simple element, the air properties are defined using this element with properties including density and far field velocity.

4.3 Utility Objects

- Frames and Triads - To orient the various structural and aerodynamic elements in spaces other than inertial, the use of both frames and triads is essential to the definition of a model using DYMORE. Frames can be defined as either fixed in the inertial space with a given orientation or as a moving frame attached to a component of the model. Triads are required to orient each of the components within the model including defining the axis of rotation for the various joint components.

- Dead Loads - All of the non-aerodynamic loading in the stop-fold model is applied via dead loads. These loads are simply forces or moments described by either a prescribed time function or a harmonic funtion. The rap test was conducted using a force dead load and the initialization of the model is accomplished with an applied torque on the shaft similar to the input from a drive

system.

- Prescribed Displacement - To specify the motion between two bodies the prescribed displacement can be applied to a body or joint. The prescribed displacement can also be used to specify rotation as is the case for the fold joint.

- Copy - To simplify model creation, DYMORE allows the use of a copy command to duplicate identical components. The copy command is especially useful in creating things such as rotor blades. The copy command functions by specifying the base frames for objects to be copied to and giving components set to be copied a "tag" that the copy command will recognize and copy into the new frame.

- Sensors - DYMORE has different sensor options dependent on the type of object being sensed. The primary use of sensors for the stop-fold model detect relative rotations between objects and to detect displacements.

- Signal Analysis - After collecting data from a simulation run, DYMORE permits basic signal analysis on the output of the sensors. The only use of this signal analysis in the stop-fold model is to apply a Fourier Transformation to extract the primary frequencies of response.

CHAPTER V

MODEL DEFINITION

5.1 Reference Configuration

To facilitate the overall analysis and to clearly see the effect that the adjustment of properties had on the dynamic response, a baseline reference configeration needed to be established. Most of the details were provided in the Bell Helicopter final reports on the stop-fold, but there were many quantities that required assumptions or simplifications.

Most of the assumptions are contained within the blade properties; but some, such as the dimensions and mass properties of the pylon, were also assumed values.

5.2 Frames of Reference

To define and orient the stop-fold model two primary frames were used for the definition of each blade as well as both the inertial frame and a local hub frame. Each blade requires the definition of its own local frame with the x axis aligned down the blade, the y axis in the chordwise direction, and the z axis normal to complete the right handed system. This fixed frame does not rotate with the blades but is instead used for the initial configuration of the model. The second frame associated with the blade is a moving frame which, while initially aligned with the fixed frame, remains attached to the blade as it rotates within the inertial frame. The moving frames are used primarily as a means to measure the airloads within the local blade system as opposed to including the 1/rev component inherent to the non-rotating system.

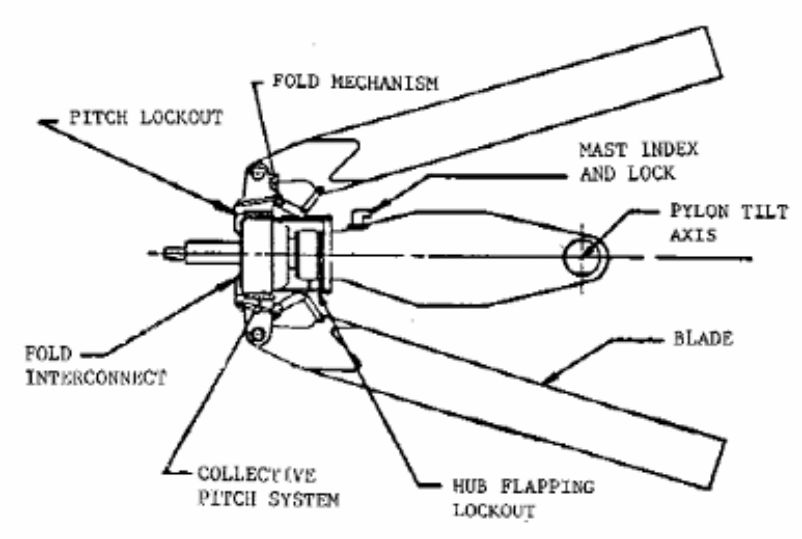

Figure 2: Model Sketch

5.3 Blade and Hub Assembly

To model the hub and rotor blades only minimal assumptions were made about the composition of these elements. Using the test model information from the original Bell Helicopter wind tunnel test[1], information about most of the blade structural properties could be obtained. These properties included the mass per unit length, beamwise and chordwise stiffness parameters, and the blade torsional stuffness. In order to form a complete DYMORE model, the blade mass moment of inertias were approximated using a representative dummy blade with a chord of 14 inches to match the test model. The provided properties began outside of the cuff just at the fold joint and were sufficient to define the entire blade element but not the hub or yoke elements. By using a DYMORE beam element and an associated lifting line the rotor blades could be properly defined.

The hub itself is approximated as a rigid body rather than a beam or surface element for two reasons: Primarily, there were no structural data available for the non-blade components of the blade-hub assembly. Secondarily, this hub configuration

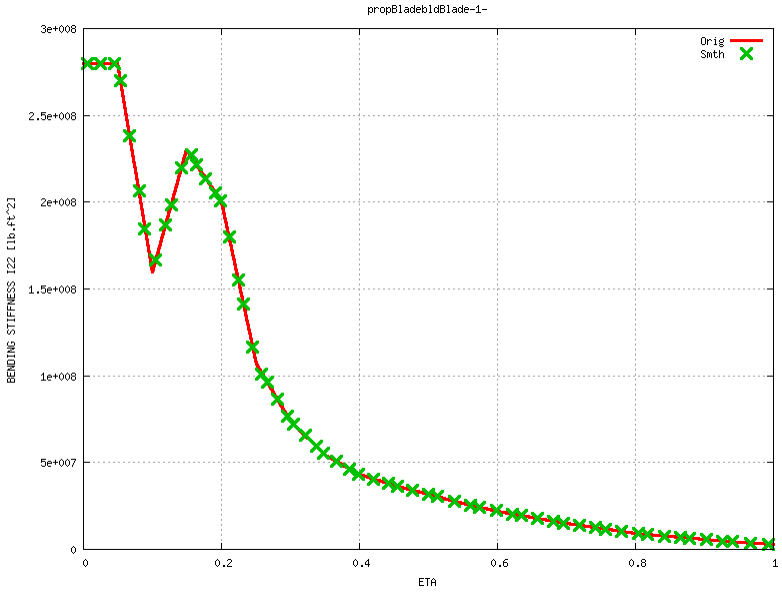

Figure 3: Blade Bending Stiffness I_{22}

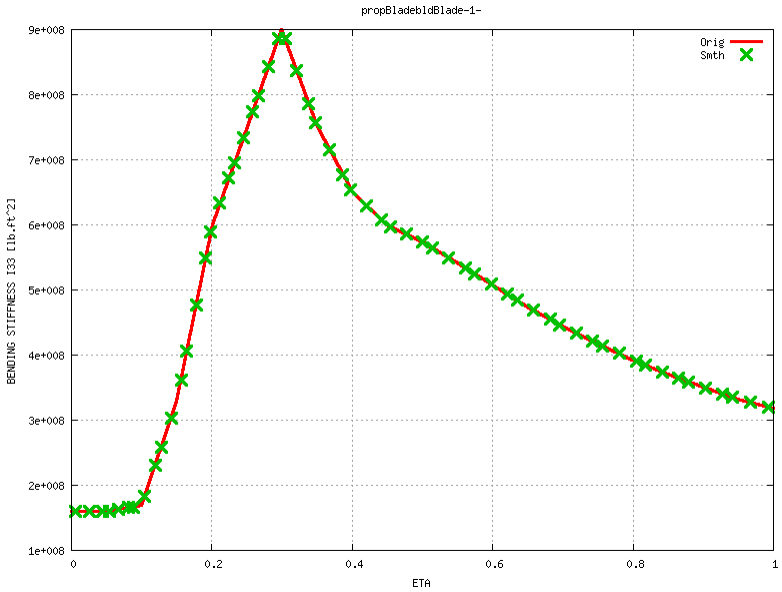

Figure 4: Blade Bending Stiffness I_{33}

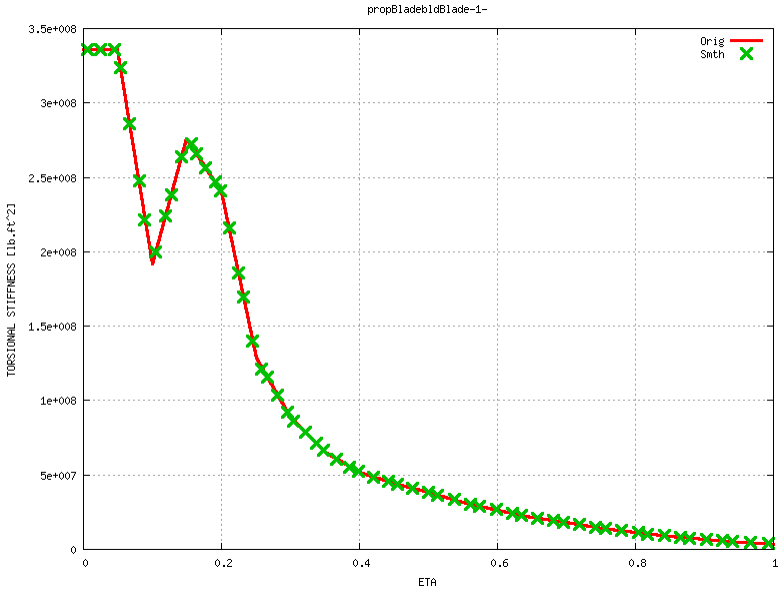

Figure 5: Blade Torsional Stiffness

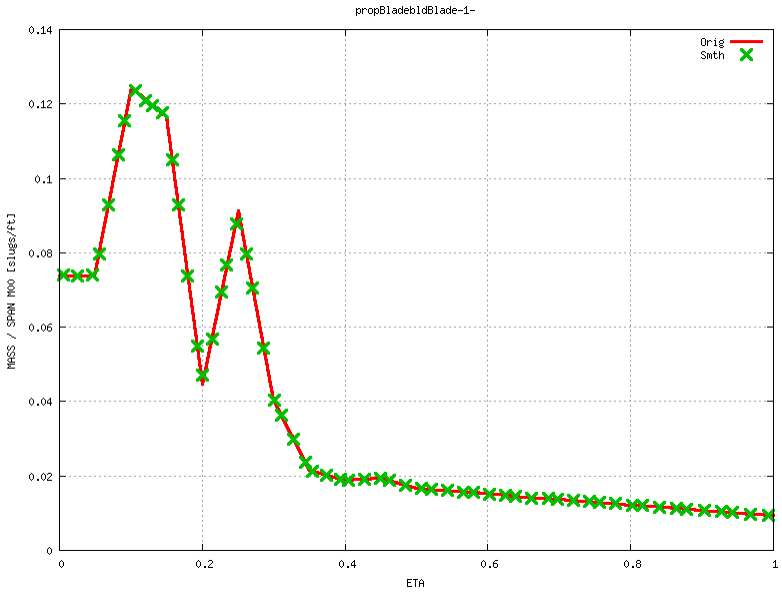

Figure 6: Blade Mass per Unit Length

permitted flapping at the midpoint of the hub as a teetering-type configuration. Typically, when flapping is accommodated by a hinge, the hub and yoke can be expressed as rigid bodies by assuming that deformations will be accounted for in the blades and at the hinge itself.

During the conversion sequence the original stop-fold model called for a flap lockout to engage to limit the flapping motion of the blades. Rather than simulate the lockout procedure the DYMORE model assumes the flap lock is always engaged. The resulting dynamic effect on the rotor should be negligible considering the lack of flapping motion prior to the conversion sequence. The hub spring value (with lockout engaged) of 4500 ft-lb/deg is included via two torsional springs connecting the hub to the shaft[1].

5.4 Pylon and Ground Mount

Both the pylon and ground mount assemblies are completely composed of rigid bodies and springs. Similar to the hub assembly, there were no applicable data for these components to model them as flexible beam elements but also the dynamic effects were assumed to be captured by tuning the spring components to generate appropriate natural frequencies. This is considered an appropriate approximation when noting the original scope of the model: to capture dynamic trends rather than accurately simulate an exact previous stop-fold test model. Initial spring values for the baseline model were arbitrarily chosen as extremely high stiffness (on the order of 10,000,000 ft-lb/rad) to be evaluated and modified during model testing.

The spring elements involved in the pylon and ground mount assemblies only include two torsional springs acting as a mount for the pylon. These torsional springs are associated with a universal joint aligned to allow relative rotations about the 2 axes normal to the shaft direction. Beneath the universal joint is a revolute joint used to permit the rotational motion of the rotor. The ground boundary condition below

the revolute joint constrains both translation and rotation in all directions to permit motion only to be dictated

In order to apply a torque to the shaft, DYMORE required mass and inertia properties to be defined. A simple assumption was made that the shaft was a steel rod with a total mass of 1.325 slugs. Moments of inertia were based on a perfect solid cylinder 4 feet in length and 1 inch in diameter.

5.5 Control System

Both the initial stop-fold model and the current DYMORE model utilize a swash-plate pitch link assembly to control blade pitch. The DYMORE model can easily be modified to accommodate cyclic pitch but is currently set up only for collective pitch. This is an accurate representation of the airplane flight mode for which the dynamics are being analyzed.

The actual swashplate is a prismatic joint rigidly attached to the rotating shaft with the only degree of freedom being translation along the shaft direction. This translational motion is transmitted up the pitch link to the pitch horn and generates the collective blade pitch. In order to alter the model to accommodate cyclic pitch the prescribed displacement at the prismatic joint for each of the swashplate "arms" would be necessarily different.

The entire control system stiffness is approximated by a single linear spring at the midpoint of the pitch link. This allows relative blade pitch motion outside of the prescribed motion from the swashplate. This single spring is the primary driver for the torsional blade mode and, in similar methodology to the ground mount springs, was initially chosen at a very high stiffness value and later tuned to be more representative of real values.

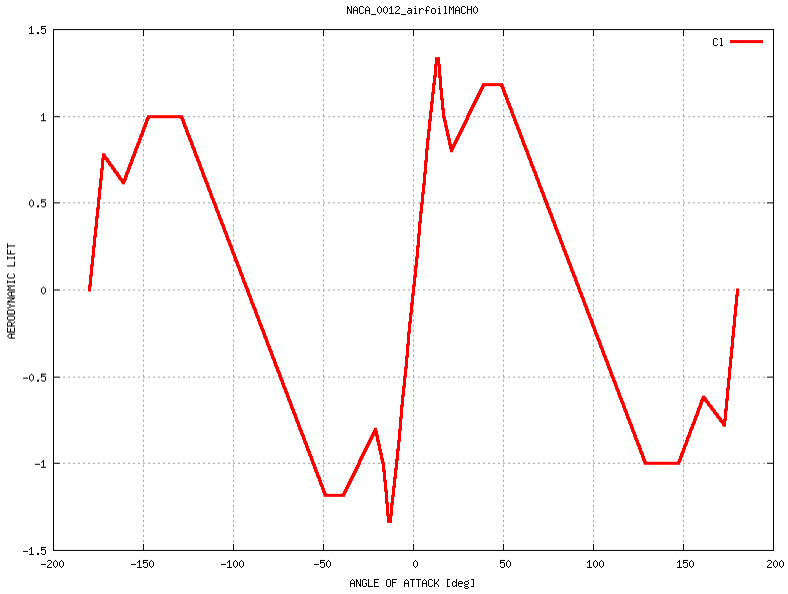

Figure 7: NACA 0012 Lift vs Angle of Attack

5.6 Aerodynamics

The original stop-fold blades consisted primarily of NACA 64-208 airfoils [1]; but, as data for this particular airfoil were unavailable, a necessary approximate airfoil was used in its place. Instead, data for a NACA 0012 airfoil was used to represent the aerodynamics of the blade. This airfoil data, shown in Figures 7 – 9, was used for all blades and all segments of each blade. By using discrete data points, as opposed to a simple lift curve slope approximation, it is possible to more accurately describe and model the stall effects as the blades are feathered sharply to bring the rotor to a stop.

The lifting lines associated with each blade are defined by a collection of airstations at which aerodynamic loads are computed and then applied to the body they are associated with. Since the structural data were provided as 20 discrete points along the radius of the blade, 20 air points were placed in conjunction with these structural data points.

The last major component of the aerodynamic model was the inflow. DYMORE

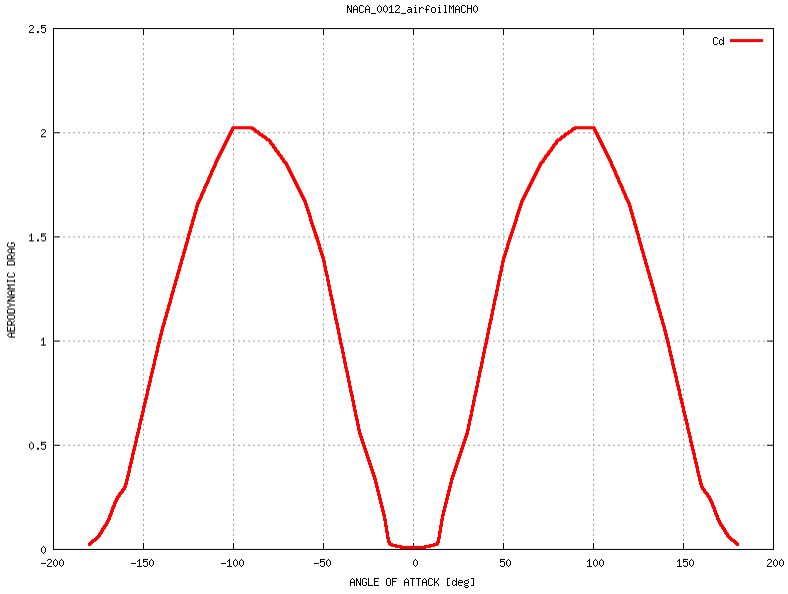

Figure 8: NACA 0012 Drag vs Angle of Attack

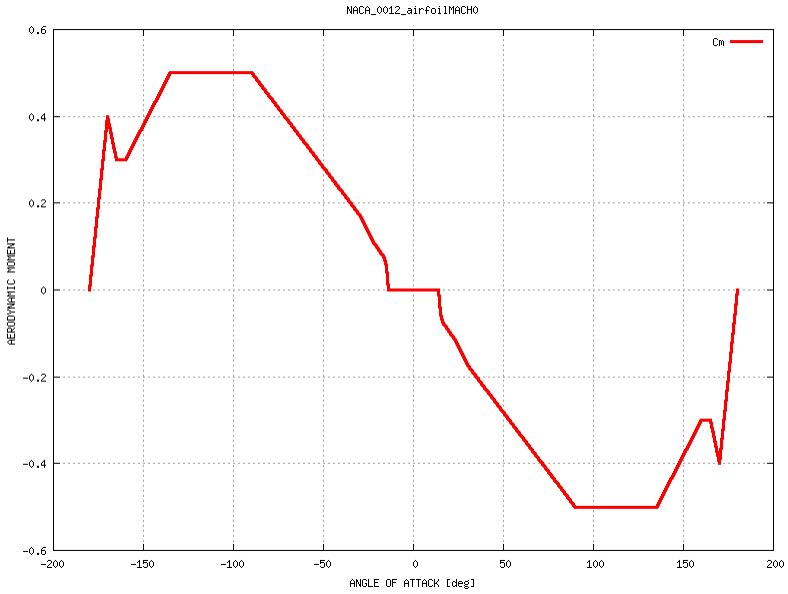

Figure 9: NACA 0012 Lift vs Angle of Attack

is capable of modeling the inflow in three different ways: a two dimensional inflow model based on the Theodorsen function, a dynamic inflow based on unsteady flow over over the rotor disc, and an exterior code Free Wake developed at the University of Maryland. Since the overall aerodynamic model consisted primarily of discrete data points along the blade and a table-lookup type model for the aerodynamics, the two dimensional inflow model made the most sense to apply to this aerodynamic representation.

CHAPTER VI

METHODOLOGY

6.1 Natural Frequencies

To evaluate the various natural frequencies of a system, DYMORE is capable of orthogonal decomposition to return these frequencies. However, this is only available if all elements are composed of beam-type elements. Since the stop-fold model includes several rigid bodies to approximate the structure, using orthogonal decomposition is an impossible way to identify all of the primary natural frequencies. To overcome this deficit, a more approximate method was designed around the engineering approach to identifying natural frequencies in real systems: a rap test.

When trying to identify natural frequencies in real systems, a rap test is commonly performed on various components. The test itself consists of attaching accelerometers to a component and striking it to excite some amount of motion. This motion can be captured with the accelerometers and, using a Fourier Transform, can be analyzed to extract the natural frequencies of vibration.

To best model this test, first sensors were set up to detect either displacements or rotations on the model. A displacement sensor was attached to the center of the hub to identify pylon modes, a rotation sensor was attached at the feathering joint to identify blade torsion and control system modes, and another displacement sensor was attached at the tip of the blade. Normally multiple accelerometers would be attached to any given component to get a collective look at the mode shape to aid in identifying which mode was being excited but for the purpose of this model these single sensors could identify the appropriate modes.

Additionally, in a real system the accelerometers detect "noise" from other modes

being excited by the rap test. By using DYMORE for this application, we are in a sense using a perfect system: by striking in the x direction we are assured no component of the strike will be in the y or z directions.

The target values for the tuning of these springs needed to be experimentally obtained to match the frequency values provided in Reference [1]. The primary target values considered were the pylon yaw at approximately 10.7 Hz and wing torsion at 6.2 Hz, as these two modes represented the degrees of freedom at the base of the pylon mount. The other modes such as the cyclic and collective rotor modes were not tuned to specific values by adjusting blade properties as the properties were already defined.

6.2 Simulation

To complete the overall analysis of the model, a full conversion sequence was simulated from airplane mode to a stopped configuration. As an overview, to initialize the model an applied torque of 8667 ft-lbs will bring the model to its nominal airplane mode of 458 RPM. Once this steady-state operation mode is reached, the rotor can be effectively declutched from the drive system simply by removing the applied torque. This reduction in torque, coupled with an increase in the collective blade angles, results in an aerodynamic moment countering the spin of the rotor effectively bringing it to a stop. A prescribed rotation at the fold joint is used to actually fold the blades along the pylon and when they are fully folded, the simulation is over.

6.3 Initialization

In order to begin analysis, the stop-fold model needed to be brought up to its nominal airplane mode operating state of 458 RPM. The final Bell Helicopter report cited a torque value of 104,000 in-lb (or 8,667 ft-lb)[1] for the design cruise in fixed wing operation. Using this suggested value on the stop-fold model resulted in a rotational speed of 47.74 rad/s, or approximately 456 RPM. This torque value was applied at

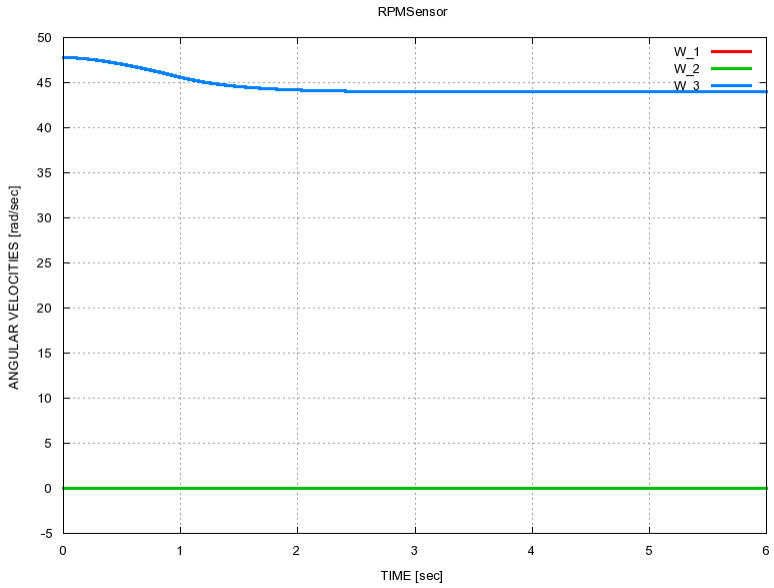

Figure 10: One Second Linear Declutch

the base of the shaft where a real drive system would engage the rotor.

6.4 Stop Sequence

6.4.1 Declutch

After initialization, the simulation of declutching the rotor was approached in two different fashions to see if the methodology had any effect. First, the declutch was simulated by linearly reducing the torque from its initial value of 8,667 ft-lbs to zero over a period of one second. Figure 10 shows the resulting trend in the rotational motion of the rotor.

A second approach was a more sudden decrease in torque; again the reduction in torque was linear, but over a period of just 0.1 seconds. Figure 11 shows the effect of this rapid decrease on the RPM of the rotor which, when compared with the 1.0 second reduction in Figure 10, simply shows a more rapid stabilization of the neutral RPM.

After considering that the only apparent effect that the declutch rate had was the time to reach a new steady-state RPM the 0.1 second torque reduction was selected

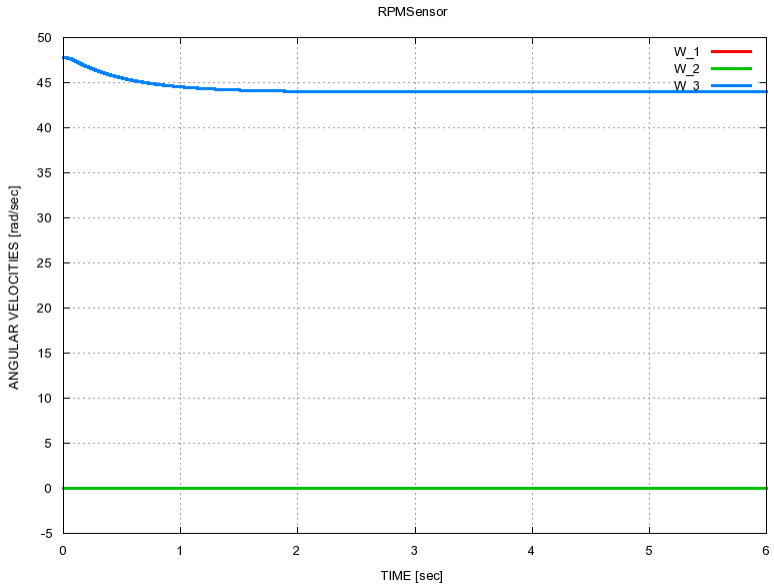

Figure 11: One Tenth Second Linear Declutch

to be what seemed more representative of a real system. The selection, however, was largely arbitrary as there seemed to be no apparent effect on the system.

6.4.2 Feathering

The actual stop portion of the stop sequence comes after the rotor has been declutched and has nearly reached its steady-state operation RPM for zero torque. The steady-state value is approximately reached in 1.0 second and this is where the feathering motion is input. By increasing collective and stalling the blades, rotor motion is quickly slowed to a near stop. The Bell Helicopter experimentally found that when the 2/3 radius was aligned with freestream the rotor came to a near stop.

Similar to the original test configuration, the stop-fold model was necessarily reindexed to accomodate the large collective range. The original twist distribution called for a root angle of 33 degrees at the neutral position, but this root angle was found to be too limiting for the purposes of this simulation. The swashplate motion was found to accomodate an increase or decrease in collective angle of approximately 60 degrees limiting the maximum root angle of attack to around 93 degrees. Even at

this maximum the steady RPM was far too high to consider the blades stopped. To facilitate the analysis portion, the blade was arbitrarily reindexed 40 degrees higher than the original listed neutral configuration for a root angle of 73 degrees with zero swashplate motion.

To actually bring the rotor to a stop, the swashplate was moved incrementally to see the resultant steady-state RPM to find the correct displacement. Using the suggestion of aligning the 2/3 radius with freestream as a starting point, it was quickly established that a final swashplate displacement of 6 inches, corresponding to a root angle of 113 degrees, limited the steady-state RPM to under 10, the limit for indexing the mast and halting the rotational motion. This position aligned a segment just outboard of the 2/3 radius point with freestream.

6.5 Folding

Due to difficulties in modeling an exact mast index tool and with consideration to its isolated effect on the overall model, the actual action of locking the mast was neglected. The rotor, after being brought to a near halt (under 10 RPM [1]), would normally have a mast lock engage, creating a sudden stop and increase in torsional loads on the mast itself. The engagement of this lock would also potentially excite a lead-lag motion of the rotor blades about the hub center. It should be noted that this effect is not present in this analysis.

To model the folding motion and look at the resulting loading and motion, an entirely separate but nearly identical model was created. The only difference between this secondary model and the primary simulation model is that the previously free revolute joint that allowed the shaft torsion was locked to reflect the engagement of the mast index. The models are identical in every other aspect. The act of folding was the simple use of precribing a rotation about the fold joint to lay the blades back along the mast.

CHAPTER VII

RESULTS

7.1 Model Configuration

Figures 12 and 13 are visual renderings of the final DYMORE stop-fold model used for this project. Figure 12 shows the model in its reference configuration while Figure 13 is a partially folded view to demonstrate the folding capability.

7.1.1 Swashplate Pitch Relationship

Once the model had been completed, the relationship between swashplate motion and collective blade pitch remained unknown. To resolve this, a simple simulation was performed to incrimentally move the swashplate and measure the resulting relative blade pitch. The result, shown in Figure 14, is a nearly linear relationship. There is a small amount of nonlinearity because the swashplate is translating while the pitch arm must rotate about the feathering joint.

7.1.2 Spring Stiffness

Before the rap test was conducted, dummy values for the spring stiffness in the pylon mount and pitch link were inserted as 10^{10} lb/ft. The hub spring was prescribed[1] as 4500 ft-lb/deg and was not adjusted. Using the rap test methodology and taking note of the resulting primary frequency in the Fourier transform it was possible to adjust the spring stiffness to achieve the target frequency values for both the pylon yaw (10.7 Hz) and wing torsion (6.2 Hz) modes corresponding to the rotation about each of the mount axes.

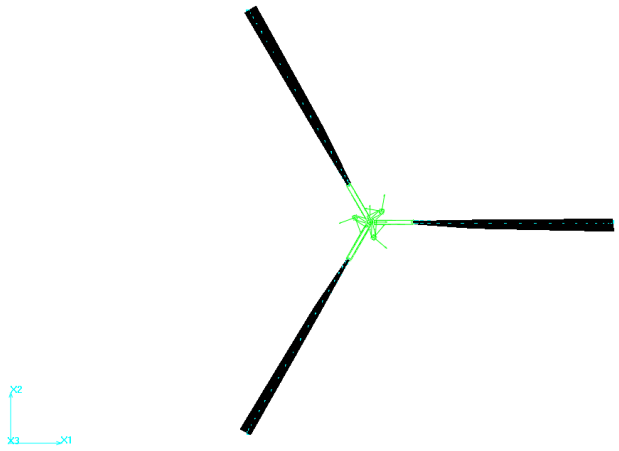

Figure 12: Final DYMORE Model in Deployed Configuration

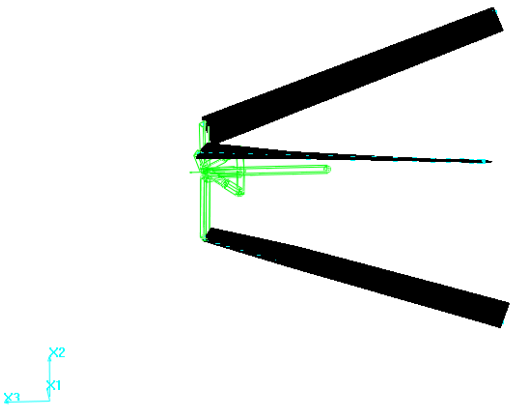

Figure 13: Final DYMORE Model in Semi-Folded Configuration

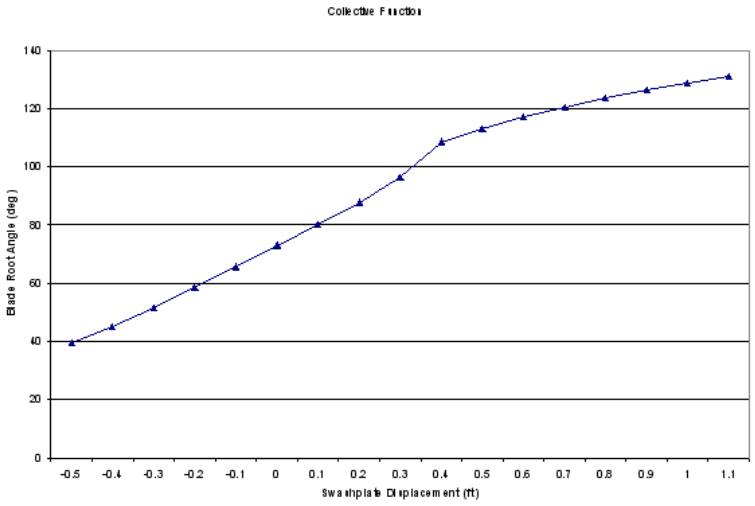

Figure 14: Swashplate Deflection vs Change in Root Angle

7.2 Feathering Rate Study

Various rates of feathering were tested with regard to their effect on the RPM, various displacements, and airloads. Feathering rates can always be limited by actuator power, but with a virtual simulation there are essentially no limits to the rates regardless of feasibility. Feathering rates here are expressed in terms of the total time from airplane cruise to fully feathered. The total swashplate travel is 0.7 feet from -0.2 up to 0.5 corresponding to a root angle change of 54 degrees from 59 degrees at cruise to 113 degrees at feathered.

For each of the feathering rates explored, the model had already been initialized to the airplane mode nominal RPM of 458 with the correct applied torque. At the start of the feathering simulation at $t = 0$ seconds, the rotor was declutched and allowed to windmill until $t = 1$ seconds. At this point, the feathering motion began and was allowed to run until the RPM had stabilized again near zero.

The results of the feathering rate study are presented in terms of both the rotational speed response as well as the total airloads. Figure 16 shows the effect on rotational speed that a two second feathering time has. This two second feathering time is reflective of the time to feather suggested in the final Bell Helicopter report.

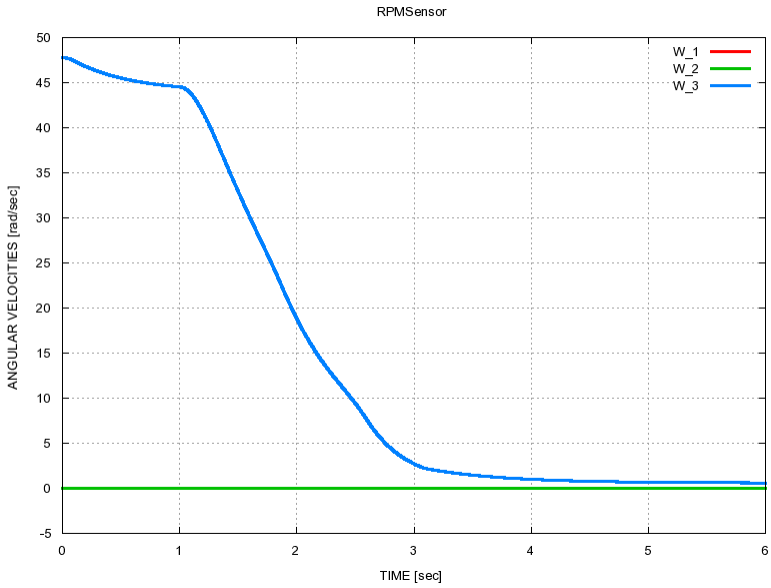

Figure 15: 1 Second Feather Rate RPM Response

Figure 19 is the same two second feathering time but shows the total airloads from this maneuver as a sum of the three individual lifting lines from each of the blades.

By comparison, Figures 15 and 18 are the results of a 1 second feathering time. The faster feathering time slows the rotor slighly faster than the 2 second feathering time but experiences a much higher transient load associated with the faster rate. Additionally, the actuator load would be dramatically higher for this rate as opposed to a slower one.

Figures 17 and 20 provide confirmation of the trend set forth by the comparison of the 1 second and 2 second feathering rates. That is, longer feathering times result in lower transient loading but stop the rotor, as expected, at a slower rate. The original design called for a fast feathering time to reduce the "buildup of oscillatory loads"[1] but this simulation did not capture any of these unstable effects. The primary benefit to a fast feathering time would be the reduction in overall drag on the aircraft after the rotor becomes unloaded. With the rotor unloaded and the blades deployed, the aircraft would pay a significant drag penalty with nothing to gain.

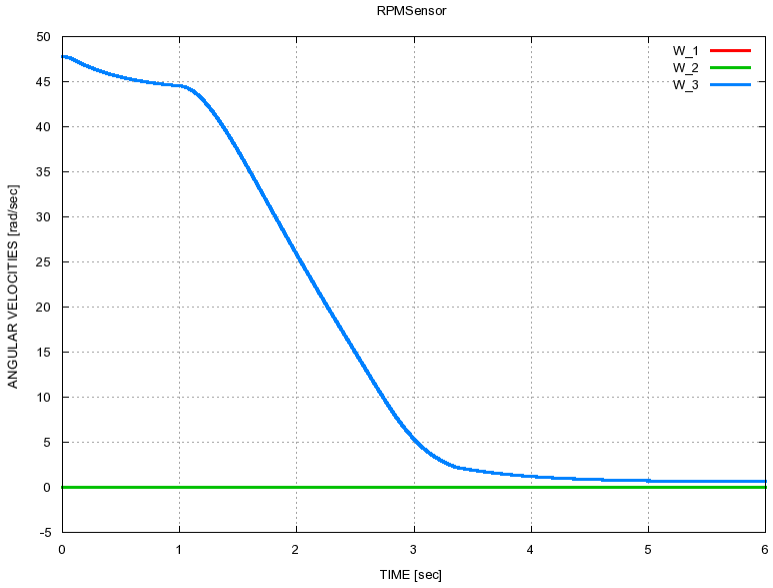

Figure 16: 2 Second Feather Rate RPM Response

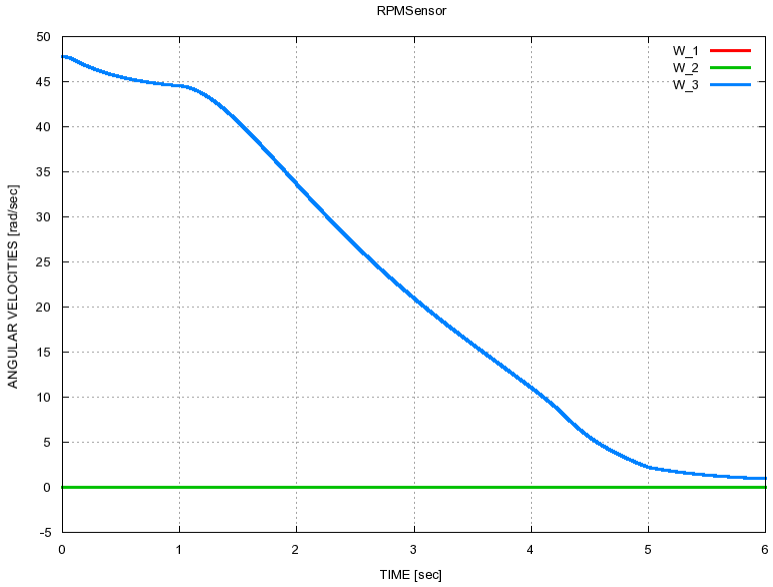

Figure 17: 4 Second Feather Rate RPM Response

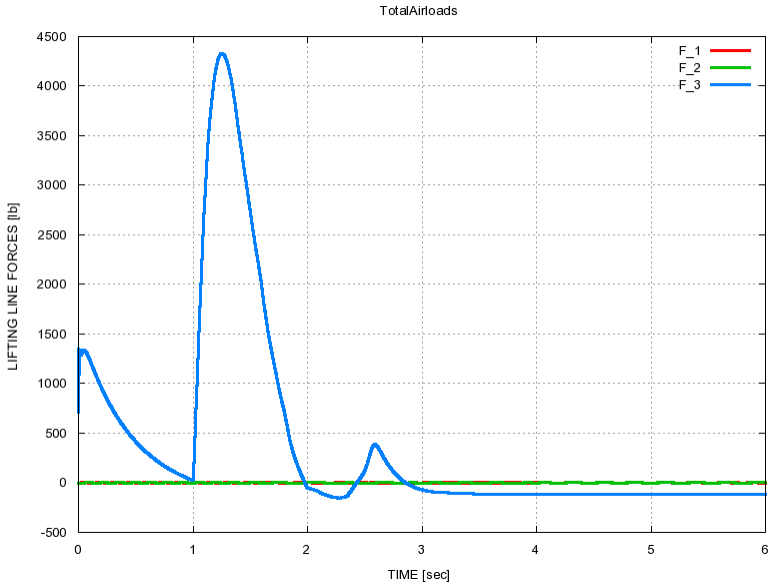

Figure 18: 1 Second Feather Rate Loads Response

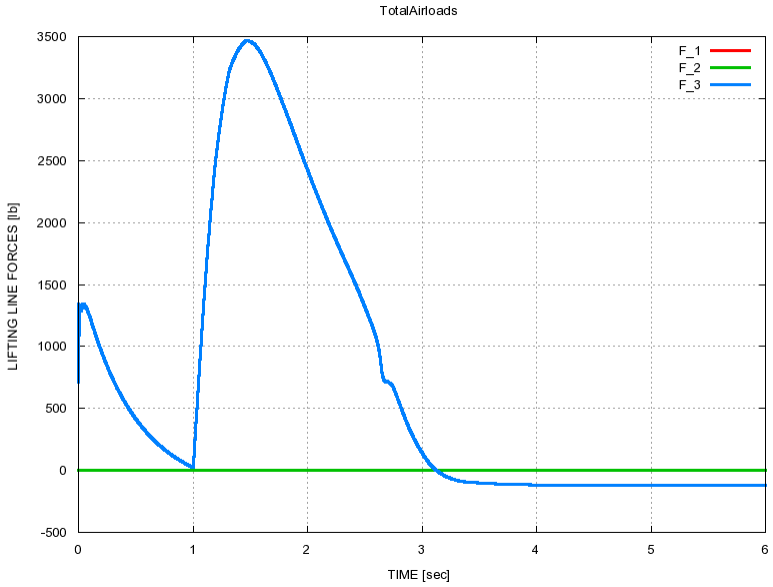

Figure 19: 2 Second Feather Rate Loads Response

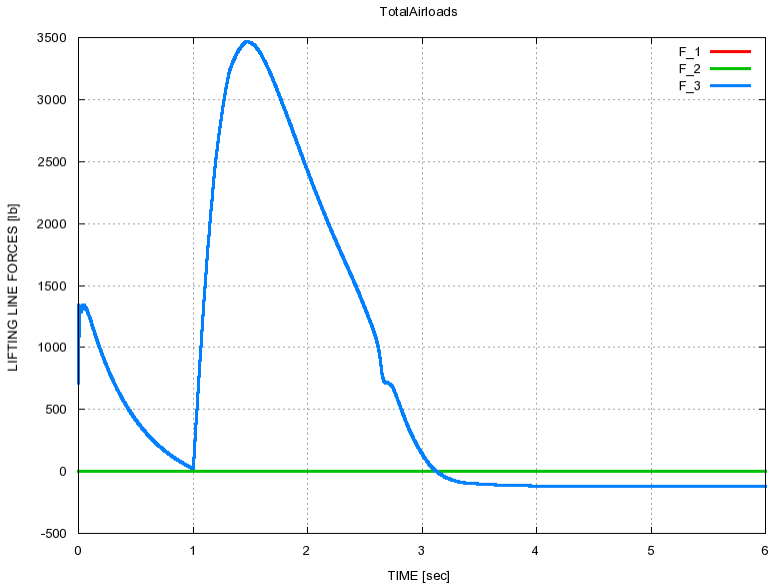

Figure 20: 4 Second Feather Rate Loads Response

7.3 Fold Rate Study

As noted in the Methodology section, the model used for the fold rate study differs from the one used for all other analysis in that it is lacking the rotational degree of freedom about the pylon. Essentially, it simulates having a perfectly locked shaft after the rotor has been stopped.

For a perfectly folded untwisted blade there would be a zero load response for the stop-fold configuration as the blades lay back along the pylon. However, this configuration has both a twisted blade and a fold axis that isn't perfectly aligned with the pylon. These two facts end up creating loading on the pylon and, over time, generate some response in the pylon itself. Interestingly, Figure 21 is the time history of the displacement at the center of the hub. From $t = 1$ to $t = 9$ seconds the blade is being folded, but not until the folding motion ceases at $t = 9$ seconds do the displacements begin to grow.

By applying a Fourier transform to the time signal the primary frequencies contained in the motion can be linked to the various modes that may be excited. Figure

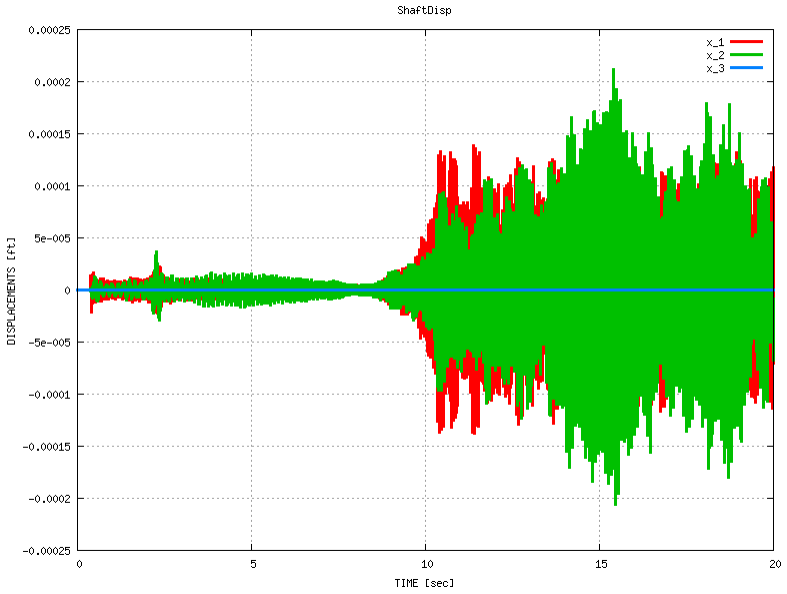

Figure 21: Hub Center Displacement with $t_{\text{fold}} = 8$ seconds

22 is a Fourier transform on the time signal from $t = 1$ to $t = 9$ seconds, the folding motion, and contains two primary frequencies. Since the Fourier transform is based on a sensor mounted to the top of the pylon, these are both modes being excited by aeroelastic interaction. More interestingly, the displacements increase dramatically after the folding motion is complete from $t = 9$ seconds on. The displacement appears bounded but, when compared to the folding motion, could be considered an unstable configuration.

The only frequency present in the transform of the response during folding of Figure 22 is 7.67 Hz. Figure 23 is the transform of the response after the folding motion has been completed and contains a large response at 10.85 Hz. For comparison, a faster feathering time of 4 seconds was simulated and similarly decomposed into its frequency components. By comparing the frequency and magnitude of response at each of the feathering rates a relationship could be established to aid in future design.

By comparing the magnitude of the displacement at the hub in both Figures 21 and 24, surprisingly the faster fold time generated a larger magnitude of response after the folding motion was actually completed. The final configuration was identical in

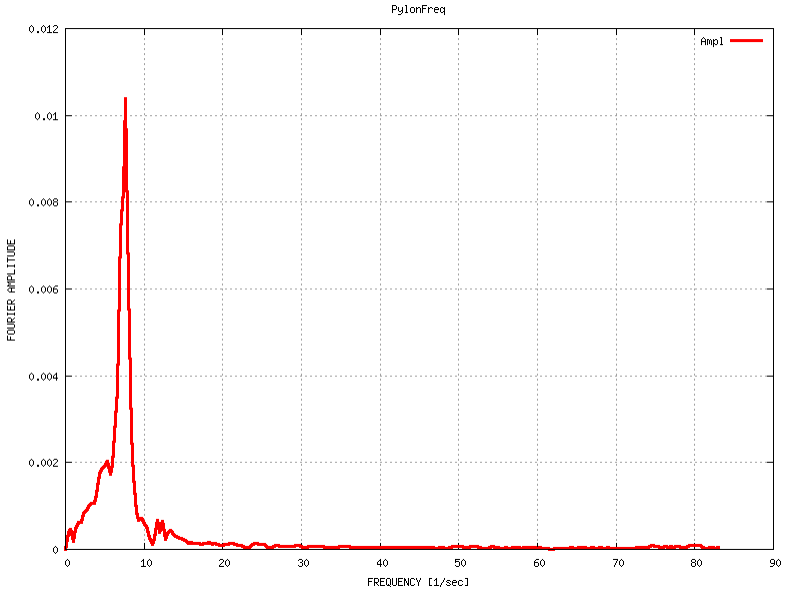

Figure 22: Fourier Transform for $t = 1$ to $t = 9$ seconds of Figure 21

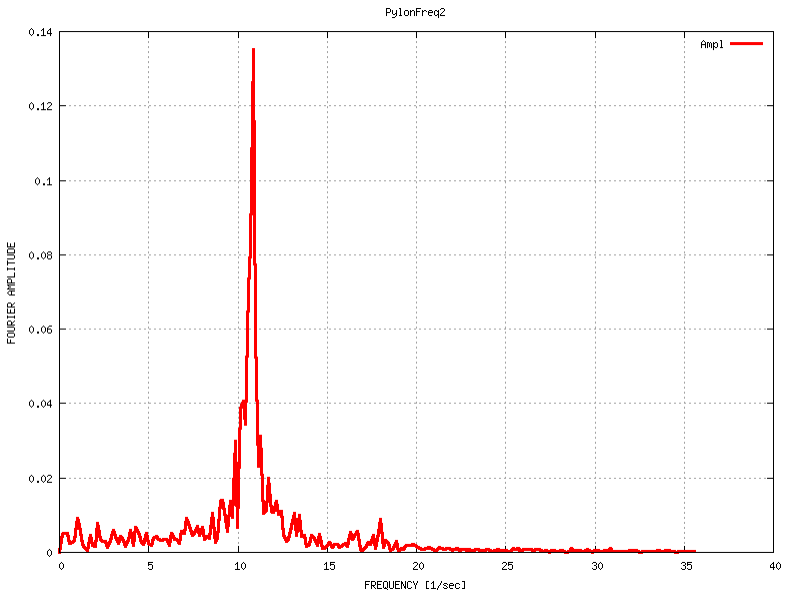

Figure 23: Fourier Transform for $t = 10$ to $t = 20$ seconds of Figure 21

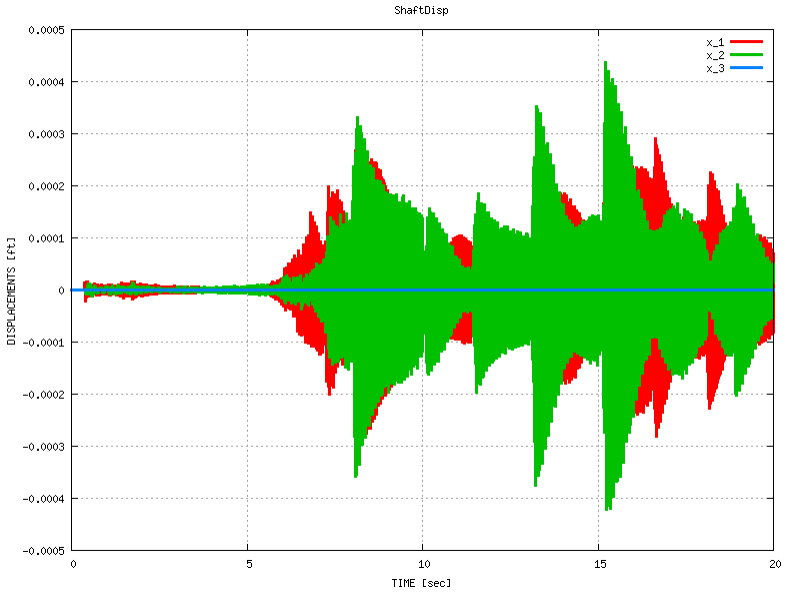

Figure 24: Hub Center Displacement with $t_{\text{fold}} = 4$ seconds

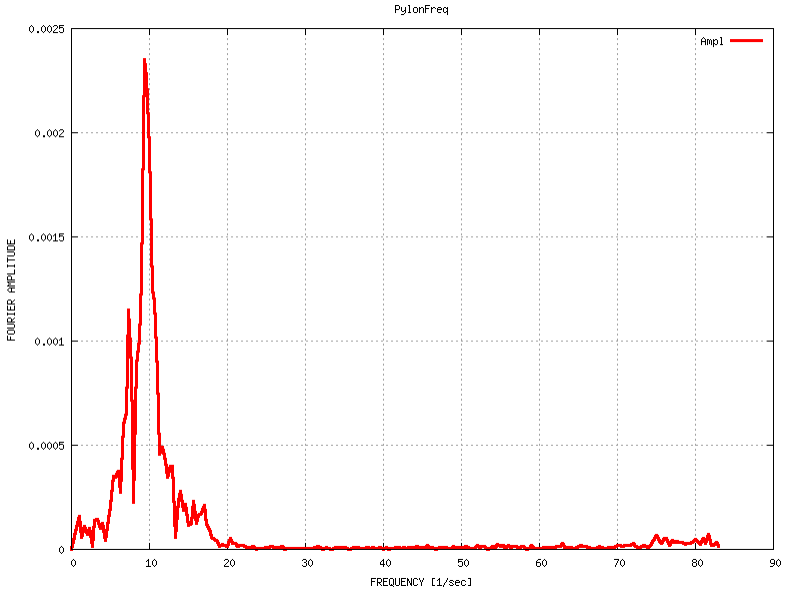

Figure 25: Fourier Transform for $t = 1$ to $t = 5$ seconds of Figure 24

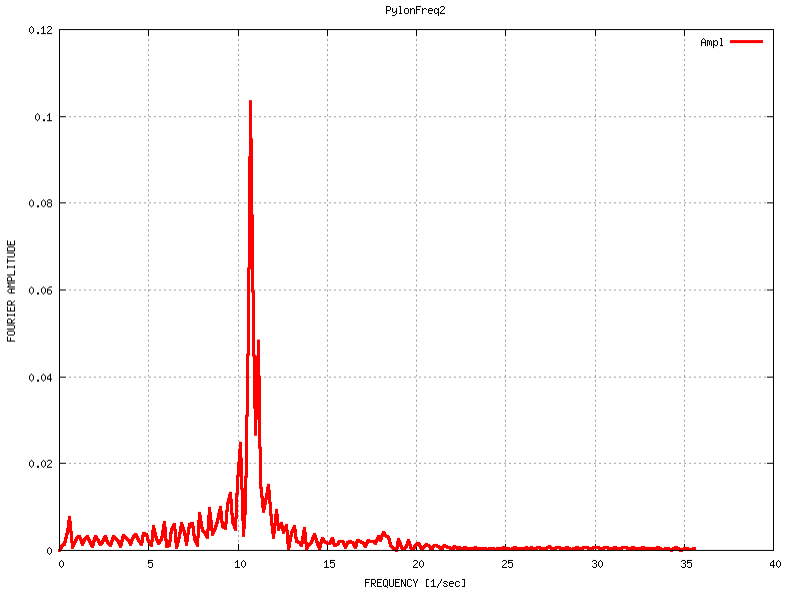

Figure 26: Fourier Transform for $t = 10$ to $t = 20$ seconds of Figure 24

both cases and yet, due to the rate of fold, the final displacements were substantially different. Whether this is a "true" dynamic effect or the result of having no structural damping in the system remains unknown, but the comparison clearly shows that there is some sort of penalty associated with the faster fold rate.

The frequency component of the motion after folding was completed was essentially identical at 10.85 Hz for the 8 second fold and 10.71 Hz for the 4 second fold. However, during the fold, the 8 second fold contained primarily 7.67 Hz signal while the faster 4 second fold jumped to 9.5 Hz. This implies a correlation between fold rate and frequency of response, and to see if this was true a much slower fold of 12 seconds was simulated.

Now by comparing Figures 22, 25, and 28, and noting that the frequency of oscillation during the fold is at 6.80 Hz for the 12 second fold, it is evident that the primary frequency of the pylon motion during folding is linked to the rate of fold: slower rates of folding equate to lower response frequencies. Additionally, but perhaps inconsequentially, the magnitude of the displacement after the fold is completed was reduced by using a slower fold time. Since the frequency of oscillation is the same at

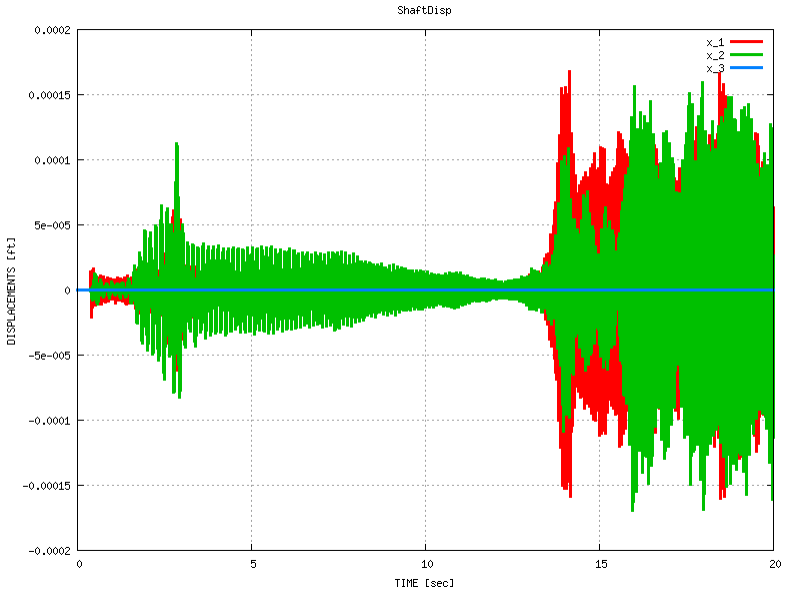

Figure 27: Hub Center Displacement with $t_{\text{fold}} = 12$ seconds

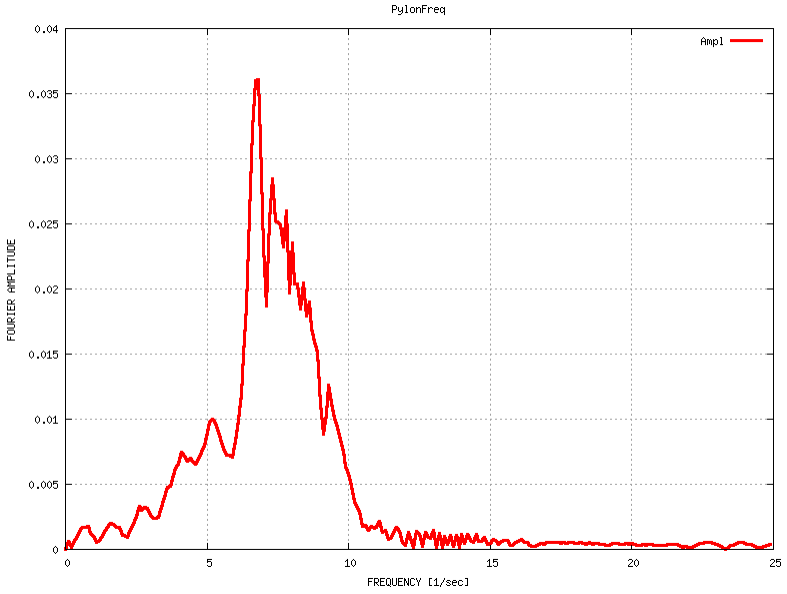

Figure 28: Fourier Transform for $t = 1$ to $t = 13$ seconds of Figure 27

10.71 Hz the same mode is being excited in each of the folded configurations but the magnitude is seemingly dependant on the rate of fold prior to achieving the folded configuration. Again, since there is no structural damping in the model it would be safe to assume that the three different magnitudes for the three different fold rates would converge to identical values with any amount of damping to diffuse some of the energy in the mode.

7.4 Natural Frequencies

One of the primary goals of the stop-fold DYMORE model was to provide a way to determine how the natural frequencies shifted as the geometry changed. By applying the rap test methodology to the pylon at various fold angles, a profile of the natural frequency trends was obtained. Figure 29 shows the shift in pylon yaw frequency over various fold angles, from 0–90 degrees, of the natural frequency. Figure 30 is the same shift but for the wing torsion mode. The wing torsion shift spanned approximately 5 Hz while the pylon yaw mode shifted approximately 8 Hz.

Each of these shifting frequencies provides an additional challenge for design purposes: They can become potenially coupled to other airframe or drivesystem modes as they undergo changes in geometry.

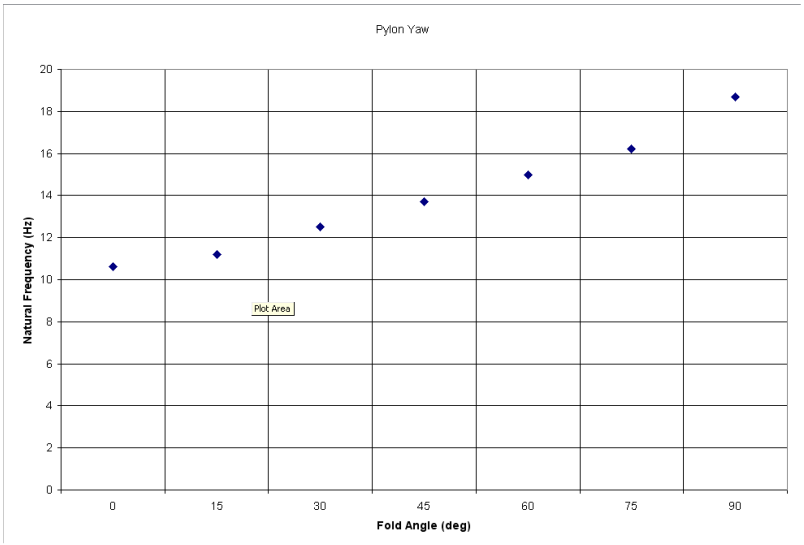

Figure 29: Natural Frequency of Pylon Yaw Mode vs. Fold Angle

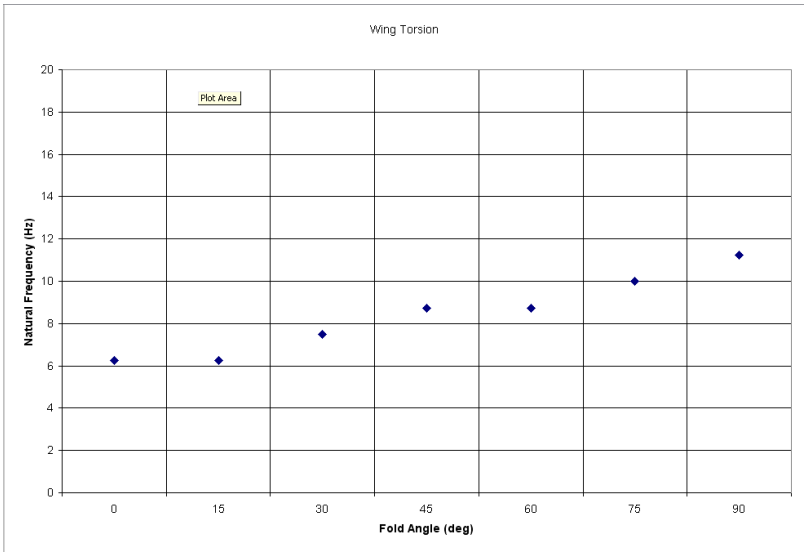

Figure 30: Natural Frequency of Wing Torsion Mode vs. Fold Angle

CHAPTER VIII

CONCLUSIONS

At its core, the stop-fold tiltrotor concept is a challenging yet feasible design that could fill a very large range of missions. The capability to operate as a conventional tiltrotor for takeoff and landing as well as making use of the high speed cruise capabilities comparable to jet aircraft make the stop-fold a highly versatile aircraft. Unfortunately, the price of this flexibility could be high.

With any morphing geometry aircraft, special attention must be given to the shift in natural frequencies as the geometry changes. These shifts can cause unstable coupling with any number of components such as fuselage modes, pylon modes, and rotor modes. The simple analysis done for this project demonstrated this shift very directly by tracking the two pylon modes as the rotor blades were folded back along the pylon.

Looking at the aeroelastic response of the stop-fold during both feathering and folding yielded interesting data, but its validity must still be taken into question. By using simplified aerodynamics on a unique problem several effects could be missing from the results. Even if the wing had been present, this method of analysis would not have captured the wing-rotor interference effect noted in the original wind tunnel testing[1].

Another added layer of difficulty in designing the stop-fold tiltrotor is the fact that there are two nominal RPMs in the design, one for airplane mode and another for helicopter mode. These two operational RPMs make tuning the rotor frequencies even more difficult, and to couple this difficulty with the problem of morphing geometry would become even more difficult.

Despite these challenges, the design is not an impossible one, and with the many mission capabilities the stop-fold is a design worth pursuing further.

CHAPTER IX

POTENTIAL AREAS FOR FUTURE WORK

9.1 Model Improvements

Information on the stop-fold model was far from incomplete when compared to the standards required to build or even accurately model a real system. The primary improvement to the model would be to replace the rigid body elements with beam elements complete with their structural properties. Using rigid body assumtions will naturally lump the dynamic response into the joint and beam elements as they can not accommodate deformations.

In addition to replacing the rigid bodies, the use of revolute joints and even universal joints can be an oversimplification of a complex component. DYMORE has a flexible joint element that would be more appropriate when attempting to create the most accurate model possible as this joint allows rotation and displacement in all directions but requires stiffness and damper inputs for these six degrees of freedom.

Currently, the only source of damping for the stop-fold model comes purely from aerodynamics. The structure, undamped, would vibrate infinitely while a real system clearly would not, so a logical improvement to the model would include structural damping and damping in the joints.

One other potential improvement that may be more of a simple change is analysis of different number of blades. Due to the construction of the model using a copy command, the number of blades could just as easily be four or even five. Clearly space would become an issue for a pitch arm assembly and would limit the number of blades but the potential is there to modify the number of blades in a very simple and efficient manner.

The stop-fold aerodynamic model was a very basic aerodynamic interface using both approximate inflow and approximate airfoil data. The primary, and easiest, method of improvement would be to obtain true data for whatever airfoil was chosen to be used in the model. The original stop-fold concept utilized an NACA 64-208 airfoil[1] for which data are no longer available. As a substitution, data for an NACA 0012 series airfoil were used, but this selection was largely arbitrary.

The second improvement to the aerodynamic model, and one that could be considered essential, would be using a CFD code paired with DYMORE to obtain realistic aerodynamics. For steady-state operation in either helicopter or airplane mode a more approximate model would most likely be accurate enough, but aerodynamic assumptions begin to fail as the blades go through high stall angles in the rotor wake as the blades are feathered to stop the rotor. Additionally, assumptions break down as the fold angle of the blade approaches ninety degrees and the flow shifts from chordwise to purely edgewise flow. DYMORE is built to accommodate the coupling of a structural model to an external code. DYMORE has a specific setup to handle OVERFLOW, COPTER, or RDYNE, but is built to handle any properly formatted external read-write CFD programs.

There are a potentially large number of effects that could remain uncaptured without the CFD analysis during the stop-fold conversion sequence. As previously noted, during initial testing Bell Helicopter discovered a wing rotor interference effect that would remain uncaptured by the current approximate model. Bell Helicopter concluded that this interference effect appeared to excite, as one might expect, the flapping mode since the interference presented to the rotor as a cyclic excitation. A CFD analysis of the configuration, complete with a full wing, would be able to capture these effects and other potentially unstable ones missed by the current approach.

9.2 Integration

One of the original goals of the project was to create a model not only for initial exploration of the stop-fold concept but also to permit the integration of this basic model with an overall aircraft model. The basic model presented here would be easily integrated with an aircraft simply by replacing the grounded boundary condition at the base of the shaft with the tip of a wing. Nearly everything in the model is defined in local frames rather than inertial allowing for easy integration.

APPENDIX A

BLADE PROPERTIES

Several of the properties were chosen as constants when representative values could not be obtained or approximately calculated without more structural and material properties. The properties that varied with span, and the aerodynamic properties used, are summarized here.

Table 1: Natural Frequency Summary

Mode	Frequency
1 Per Rev, 458 RPM	7.6 Hz
Pylon Yaw	10.7 Hz
Wing Torsion	6.2 Hz
Flapping	7.7 Hz
Pylon - Hub Motion 1	12.4 Hz
Pylon - Hub Motion 2	24.0 Hz
Collective Mode IP	129.1 Hz
Cyclic Mode IP	125.9 Hz

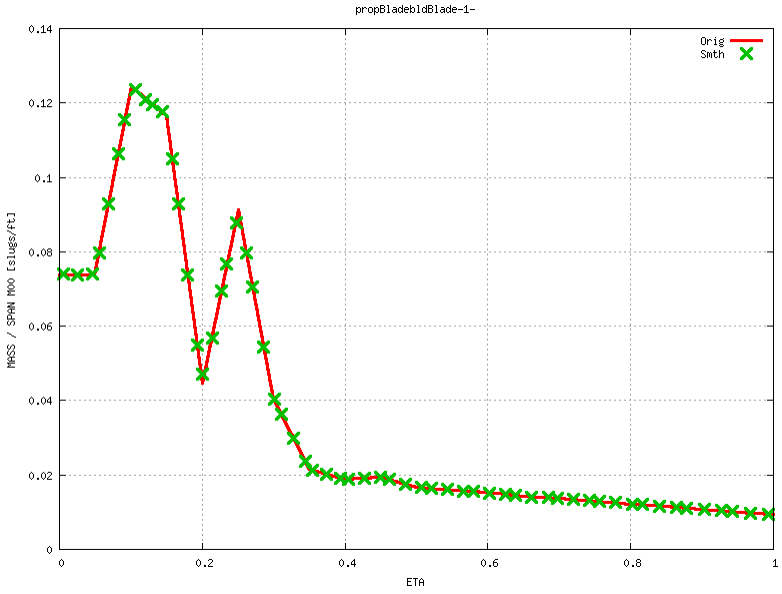

Figure 31: Mass per Unit Length

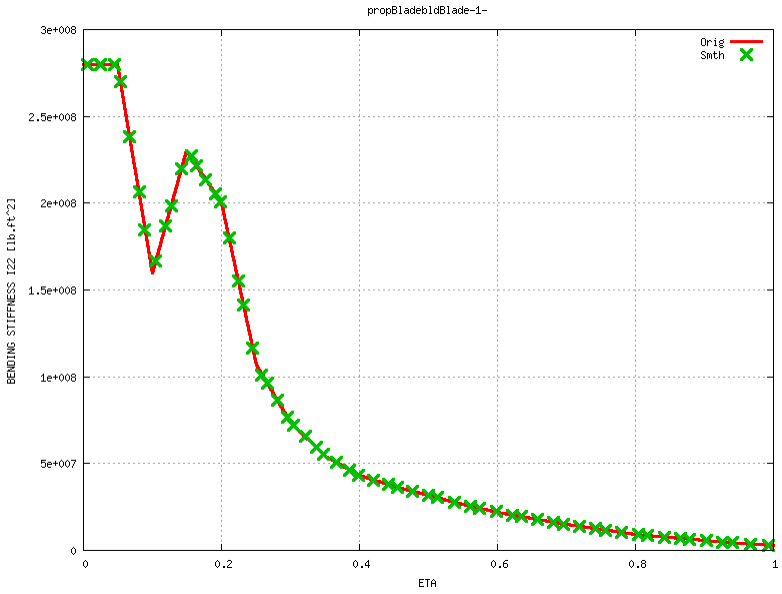

Figure 32: Beamwise Stiffness

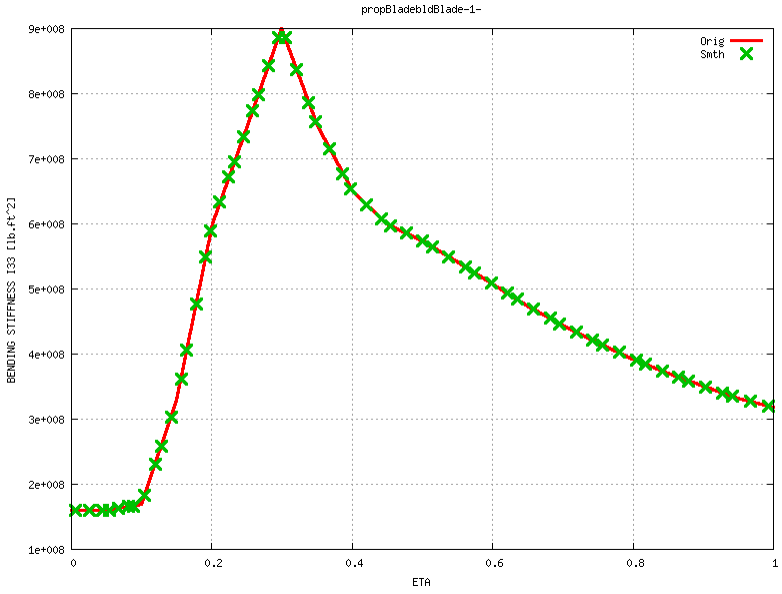

Figure 33: Chordwise Stiffness

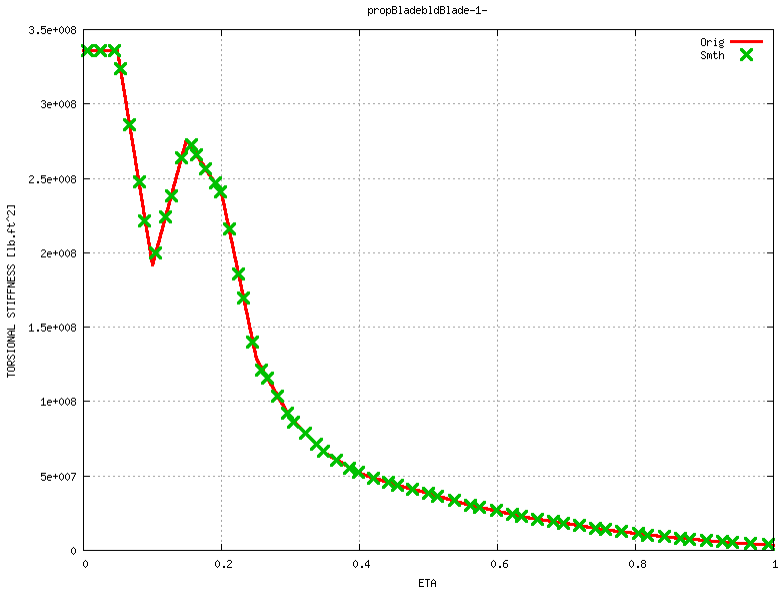

Figure 34: Torsional Stiffness

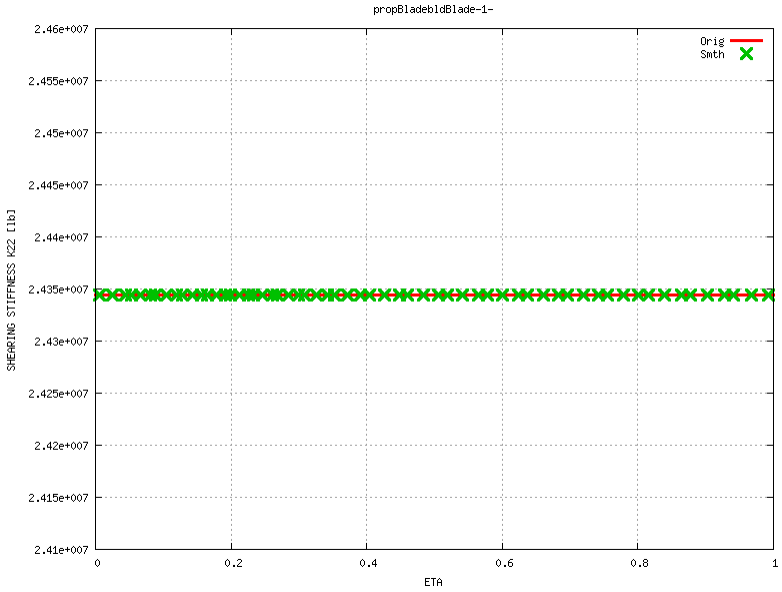

Figure 35: Beamwise Shearing Stiffness

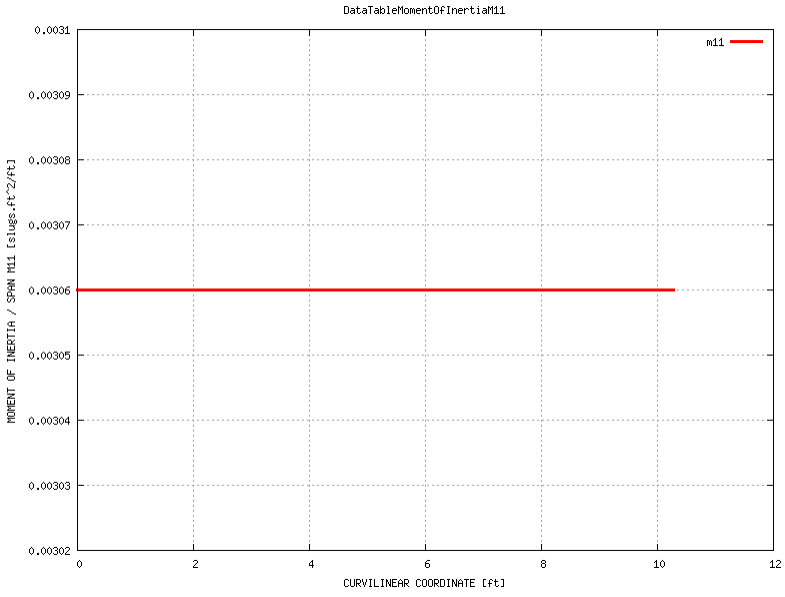

Figure 36: Sectional Mass Moment of Inertia M11

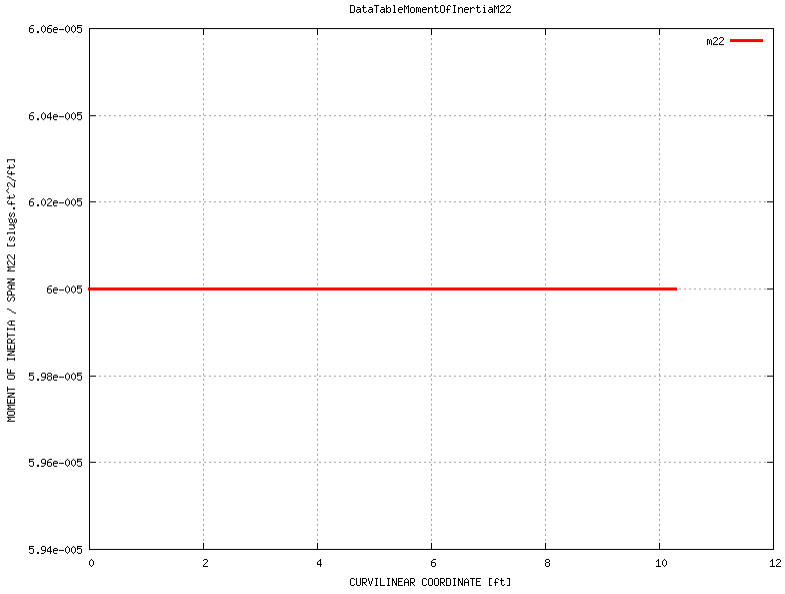

Figure 37: Sectional Mass Moment of Inertia M22

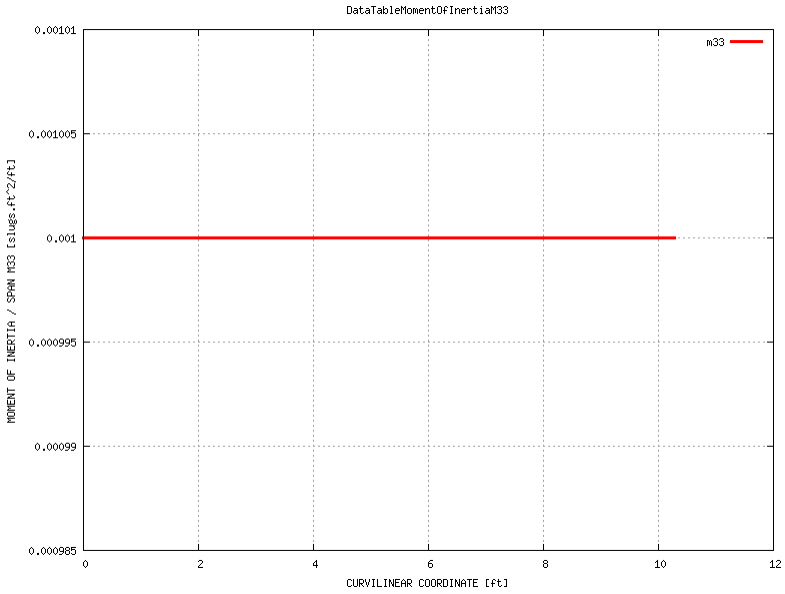

Figure 38: Sectional Mass Moment of Inertia M33

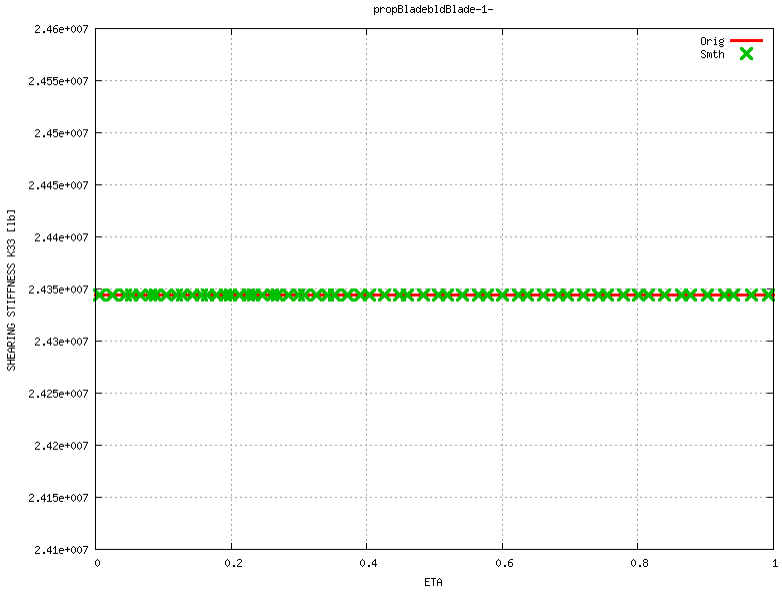

Figure 39: Chordwise Shearing Stiffness

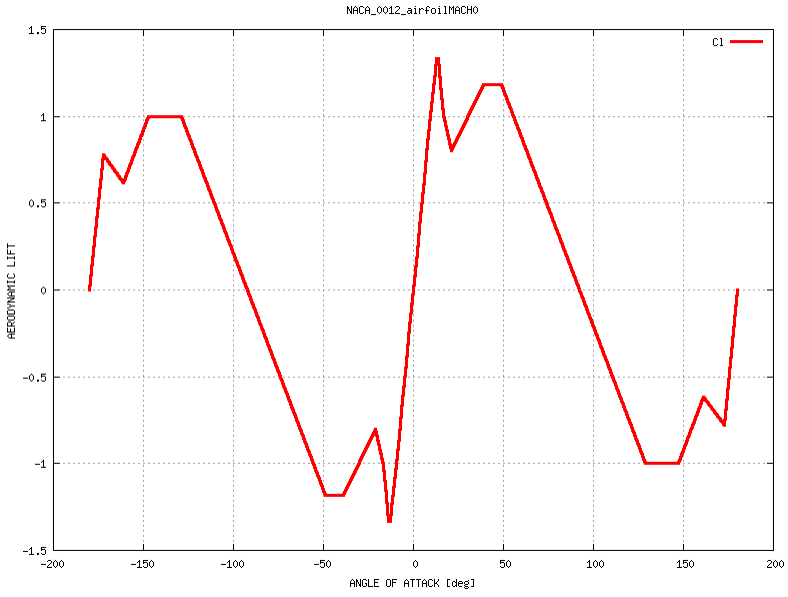

Figure 40: Sectional Lift Coefficient

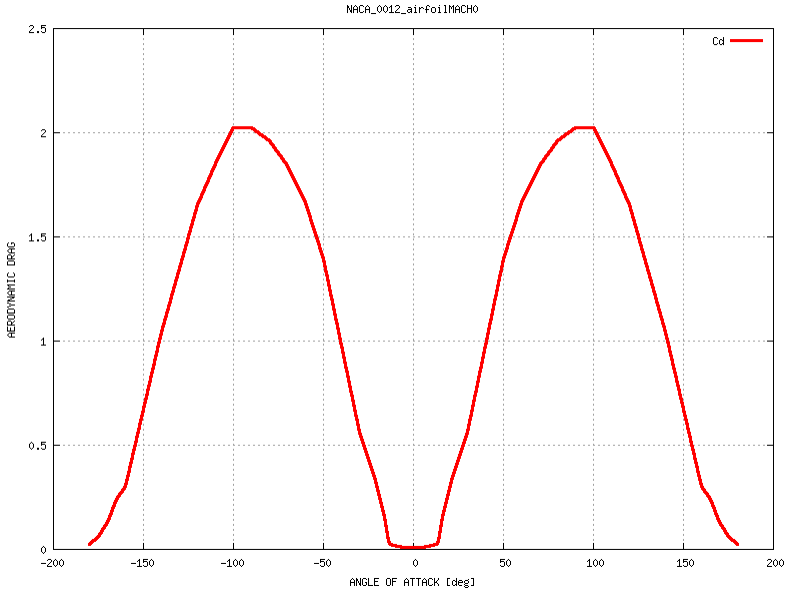

Figure 41: Sectional Drag Coefficient

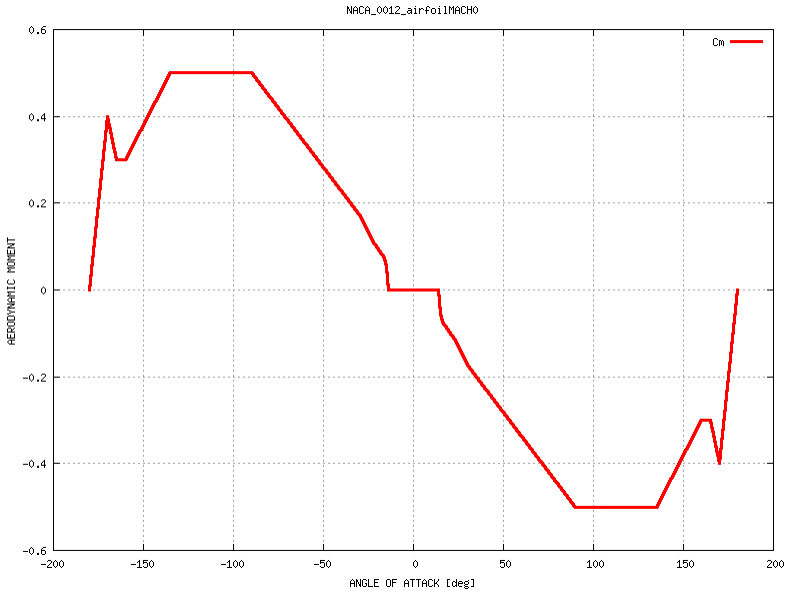

Figure 42: Sectional Moment Coefficient

REFERENCES

[1] Bell Helicopter, "Final Report - Task II, Large Scale Wind Tunnel Investigation of a Folding Tilt Rotor," *NAS2-5461*, Bell Report D272-099-002, 1972.

[2] Bell Helicopter, "Summary Report - Task I, Preliminary Design Studies NASA Folding Proprotor Program," *NAS2-5461*, Bell Report D272-099-01, 1970.

[3] Livingston, C.-L, "A Stability and Control Prediction Method for Helicopters and Stoppable Rotor Aircraft, Volume I, Engineer's Manual," vol. 1.

[4] DeTore,J. A. and Gaffey, T. M., "The Stopped-Rotor Variant of the Proprotor VTOL Aircraft," in *AIAA/AHS/VTOL Research Design and Operations Meeting*, (Atlanta, Georgia), February, 1969.

[5] Matthys, C. G., Joglekar, M. M., and Hsieh, P. Y., "An Analysis of Fixed Wing-Proprotor Interference For Folding Proprotor Aircraft," Bell Helicopter Company, AFFDL-TR-72-115, April, 1973.

[6] Talbot, P. D., Phillips, J. D., and Totah, J. J., "Selected Design Issues of Some High Speed Rotorcraft Concepts," Journal of Aircraft, vol. 30, no. 6, November–December, 1993.

[7] Friedmann, P. P., "Renaissance of Aeroelasticity and Its Future," Journal of Aircraft, vol. 36, no. 1, January–February, 1999.

[8] Bauchau, O. A., "DYMORE User's Manual," Georgia Institute of Technology, December, 2006.

[9] Ashley, H., "Update to Aeroelasticity," Applied Mechanics Update, American Society of Mechanical Engineers, New York, 1986.

[10] Fry, B. L. and Schneider, J. L., "Design Optimization of Stoppable-Rotor V/STOL Aircraft Systems," Air Force Systems Command Contract, F33615-69-C-1339, February, 1969.

[11] Yen, J. G., "A Study of Folding Proprotor VTOL Dynamics," AFFDL-TR-71-7, September, 1971.

VITA

Jeff Bosworth was born May 1^{st}, 1985, in Downer's Gove Illinois. He became a 3^{rd} generation Georgia Tech Alumnus by graduating with his Bachelor's Degree of Aerospace Engineering with highest honors in May of 2007. Jeff is currently finishing his Master's Degree in Aerospace Engineering with a special focus on rotorcraft. His current work is inspired by a Bell Helicopter design and is being guided by Professors Hodges, Bauchau, and Sankar.